Abstract: Based on the quasi-three-level system, a theoretical model of diode-laser end-pumped fundamental continuous-wave (CW) Yb^{3+}:YAG microchip lasers is proposed. The fluorescence concentration quenching effect, the temperature dependent mechanical and optical properties and the absorption efficiency of the host have been taken into account in the model. The theoretical results of the numerical calculations are in good agreement with those of experiments. The effects of the concentration of the Yb^{3+}:YAG crystal, the thickness of the Yb^{3+}:YAG crystal, the temperature and the transmission of the output coupler on the laser performance (threshold and output power) are addressed. The optimization of the concentration and the thickness for the Yb^{3+}:YAG crystal microchip laser is presented. The effects of the temperature and the pump power intensity on the optical-to-optical efficiency are discussed. The output power can be scaled by increase the working area of the laser gain medium. This modeling is not only applicable to Yb^{3+}:YAG crystal microchip laser but also to other quasi-three-level microchip lasers.

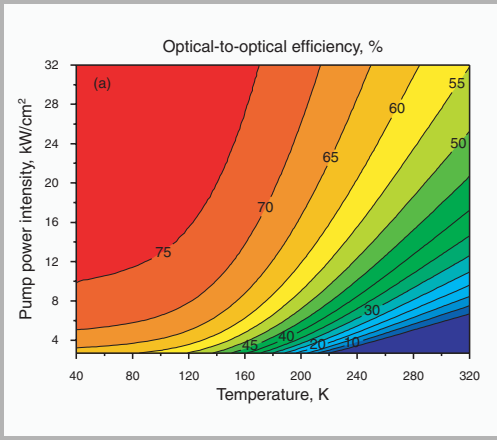

The optical-to-optical efficiency of Yb:YAG microchip laser as a function of temperature and pump power intensity.

Temperature-tuning Yb:YAG microchip lasers

Jun Dong * *and Ken-ichi Ueda*

Institute for Laser Science, University of Electro-Communications, 1-5-1 Chofugaoka, Chofu, Tokyo 182-8585, Japan

Received: 20 April 2005, Accepted: 24 April 2005
Published online: 2 May 2005

Key words: temperature-tuning; Yb:YAG; microchip; concentration quenching

PACS: 42.55.-f, 42.55.Xi, 42.70.Hj, 02.60.Cb

1. Introduction

The average output power and the beam quality in the solid-state lasers are limited by the thermally induced effects such as thermal distortion, birefringence, and the thermal stress fracture in the solid-state gain medium. Laser efficiency, however, depends on spectroscopic properties of the gain medium, such as the quantum defect and the saturation intensity, as well as the beam waist and the pump geometry. Cryogenically cooled Yb:YAG has significant potential for power scaling of efficient high-average-power solid-state lasers with good beam quality because of the material's excellent thermo-optical and spectroscopic properties at low temperature [1,2]. Laser diode pumped solid-state microchip lasers have been attractive light sources because of their compactness, high output power, high efficiency, and so on. Owing to the short gain medium length for microchip laser operation, the concentration of the gain medium should be high enough for absorbing enough pump power for high efficiency operation. Ytterbium doped YAG crystal has been an attractive gain medium for obtaining high output power and high beam quality. High efficiency laser operation of Yb:YAG lasers at liquid nitrogen temperature have been demonstrated using different geometries of Yb:YAG crystal (laser rod, and microchip) recently [3–5].

The thin disk laser based on Yb:YAG crystal has been an attractive configuration to realize the high beam quality and high output power operation [6,7]. However, the pumping configuration of laser diode pumped thin disk is multi-pass pumping of the thin disk and is very complex for designing and adjusting, the easiest way is to use single-pass or two-pass pumping Yb:YAG microchip laser at low temperature as described in [4,5]. The slope effi-

* Corresponding author: e-mail: jundong_99@yahoo.com

ciency and optical-to-optical efficiency of such laser is as high as 80% and 70%.

Recently development of the high concentration doped Yb:YAG crystal laser material has attracted a lot of attentions for high power laser applications. Compared to Nd:YAG crystal, Yb:YAG crystal laser material has several advantages such as easy growth of large size and high concentration Yb:YAG crystal, less expensive, mass production, and so on. The laser performance of diode laser pumped Yb:YAG microchip and thin disk laser has been demonstrated and high efficient operation has been achieved, the slope efficiency as high as 57.6% and optical-to-optical efficiency of 53% has been achieved with these Yb:YAG crystal as gain media. The Yb:YAG crystal laser material is a promising laser material for high power solid-state laser applications. The high concentration of Yb:YAG crystal offers another advantage for microchip laser applications. However, there is concentration quenching with increase of the doping concentration, the fluorescence lifetime of highly doped Yb:YAG crystal will decrease with concentration [2], so the concentration effect should be taken into account when highly doped Yb:YAG crystal used as microchip laser gain medium. Also the thermal population at lower-laser-level strongly depends on the doping concentration and temperature. In this paper, a laser model includes the concentration effect and temperature dependent stimulated emission cross-section and thermal population distribution of the lower-laser-level based on the rate equations was presented. The analytical and numerical solution on the laser performance (output power and pump threshold) as functions of the doping concentration and the thickness of the Yb:YAG crystal gain medium at different temperatures are presented. The numerical simulation of laser diode pumped Yb:YAG microchip laser performance is in good agreement with the experimental results. The optimization of the doping concentration and thickness of the gain medium at different temperature on the laser performance are presented for guiding to design high efficient operation of laser diode pumped Yb:YAG microchip lasers. The effects of the temperature and pump power intensity on the laser performance such as optical-to-optical efficiency are addressed. The power scaling of Yb:YAG microchip laser is predicted.

2. Laser model

Microchip lasers are formed by directly coating the dielectric films on the surfaces of the gain medium to form the laser cavities, so in principle, they are Fabry-Perot cavities. Or microchip lasers can be formed by directly coating the dielectric film on one surface of the gain medium to form the rear mirror of the laser cavity, the output coupler is separated from the gain medium which can be easily adjusted for optimizing other parameters to achieve optimizing operation of such laser system. The cavities can be treated as approximately concave-concave cavities with the thermal effects of the media taken into account or plane-concave cavities. When the pump and laser beam in the gain media are assumed to be Gaussian beams, using an M^2 factor, the radii of the pump and laser beams along the direction of the light can be written as [8, 9]

$$w_p^2(z) = w_{p0}^2\left[1 + \frac{\left(M^2\right)^2 \lambda_p^2 \left(z - z_0\right)^2}{\pi^2 w_{p0}^4 n^2}\right], \tag{1}$$

$$w_L^2(z) = w_{L0}^2\left[1 + \frac{\lambda_L^2 \left(z - z_0\right)^2}{\pi^2 w_{L0}^4 n^2}\right], \tag{2}$$

where z is the coordinate along the axis of the laser, $w_p(z)$ and $w_L(z)$ are the radii of the pump and the laser beams at z, w_{p0} and w_{L0} are the radii of the pump and the laser beams at waist $z = z_0$, λ_p and λ_L are the wavelengths of the pump and the laser, n is the refractive index of the gain media. Generally, the length of the microchip gain media is less than several millimeters, therefore, the approximation of $w_p(z) = w_{p0}$ and $w_L(z) = w_{L0}$ may be adopted.

For a laser gain media pumped by longitudinally CW incident pump power P_0, pump rate can be written as $W_p = P_0\eta_a/h\nu_p$, where h is the Planck constant, ν_p is the frequency of the pump power, $\eta_a = 1 - \exp(-2\alpha l)$ is the fraction of the incident pump power absorbed by a laser gain medium of thickness l for two-pass pumping configuration, and α is the absorption coefficient at pump wavelength λ_p. The normalized functions that describes the spatial distribution of the pump power and the spatial distribution of the laser cavity mode can be expressed as [10]

$$r_p(r,z) = \frac{2\alpha}{\pi w_{p0}^2 \eta_a}\exp\left(\frac{-2r^2}{w_{p0}^2}\right) \times \tag{3}$$

$$\times\left[\exp\left(-\alpha z\right) + \exp\left(-\alpha\left(2l - z\right)\right)\right],$$

$$\phi_L(r,z) = \frac{2}{\pi w_{L0}^2 l_c}\exp\left(\frac{-2r^2}{w_{L0}^2}\right). \tag{4}$$

The total number of the laser photons in the laser cavity is defined as $\Phi = 2l_c P_c/hc\nu_L$, where P_c is the laser power inside the cavity, c is the vacuum speed of light, and ν_L is the frequency of the laser, l_c is the optical length of the resonator.

The temperature distribution in the gain medium for end-pumped microchip laser can be written as according to [11]

$$T(r,z) = \tag{5}$$

$$= T_c + \frac{P_h\left(z\right)}{4\pi k}\left[\ln\left(\frac{R^2}{r^2}\right) + E_i\left(\frac{2R^2}{w_{p0}^2}\right) - E_i\left(\frac{2r^2}{w_{p0}^2}\right)\right],$$

where T_c is the coolant temperature at $r = R$, r is the transverse radial coordinate, k is the thermal conductivity of the gain medium, w_{p0} is the pump power beam waist incident on the gain medium, R is the radius of the gain medium or the aperture of

the cooler, P_h(z) is the heat generated inside the gain medium when the incident pump power is P_0, $P_h(z) = P_0\alpha[\exp(-\alpha z) + R_r \exp(-2\alpha l + \alpha z)]f_h$, where α is the absorption coefficient of the gain medium at pump wavelength, l is the length of the gain medium, R_r is the reflectivity of the front surface for pump wavelength, $E_i(x)$ is the exponential integral function:

$$E_i(x) = \int_x^\infty \frac{e^{-t}}{t} dt\,.$$

For the end-pumped microchip lasers, the temperature variation along the z axis is smaller than that along the radial direction, so the average temperature along the z axis is adopted. Therefore, the temperature distribution inside the gain medium can be expressed as,

$$T(r) = \tag{6}$$

$$= T_c + \frac{P_h}{4\pi kl}\left[\ln\left(\frac{R^2}{r^2}\right) + E_i\left(\frac{2R^2}{w_{p0}^2}\right) - E_i\left(\frac{2r^2}{w_{p0}^2}\right)\right],$$

where $P_h = P_0\eta_a f_h$.

Because Yb:YAG laser is a quasi-three-level system, the reabsorption of the ground state has a great effect on the laser performance, the rate equations including the fluorescence concentration quenching and the reabsorption of the ground state in steady state can be described as [10,12,13]

$$\frac{d\Delta N(r,z)}{dt} = fW_p r_p(r,z) - \tag{7}$$

$$-\frac{\Delta N(r,z) + f_{low}N_{tot}}{\tau(N_{tot})} - \frac{fc\sigma\Delta N(r,z)}{n}\Phi\phi_L(r,z) = 0\,,$$

where $\Delta N(r,z)$ is the spatial distribution of the population inversion density between upper and lower laser levels in pumped conditions, σ is the emission cross section of the gain medium at the laser wavelength, f_{low} and f_{up} is the Boltzmann factor at the lower laser level and the upper laser level of the Yb^{3+}:YAG crystal, respectively, $f = f_{low} + f_{up}$, $\tau(N_{tot})$ is the lifetime of the upper state level as a function of the concentration of the active ions and $\tau(N_{tot})$ can be described as $\tau(N_{tot}) = (0.67442 + 0.37632\exp(-C/C_0)) \times 10^{-3}$ s [2], where C is the atomic percentage of the doping ions, C_0 is the parameter that describes the concentration quenching effect in Yb:YAG crystal. The lifetime of the $^2F_{5/2}$ state of Yb^{3+} ions in highly doped Yb:YAG crystal should be governed by the sum of probabilities for several competing processes such as radiative decay, nonradiative decay by multiphonon emission and energy transfer to other Yb^{3+} ions and other impurities. The concentration quenching effect in highly doped Yb:YAG crystal may be ascribed to more-short-range mechanism of the Yb^{3+} - Yb^{3+} quenching interaction, this phenomenon plays an increasingly important role with increasing Yb ion concentration (Yb^{3+} concentration > 15 at.%). Other impurities introduced during fabrication of highly doped Yb:YAG crystal also play an important role in the energy transfer between Yb^{3+} and impurities when the Yb concentration is higher.

The corresponding equation for the total number Φ of photons in the cavity is [10,12]

$$\frac{d\Phi}{dt} = \frac{c\sigma}{n}\iiint \Delta N(r,z)\Phi\phi_L(r,z)dV - \frac{\Phi}{\tau_q} = 0\,, \tag{8}$$

where

$$\tau_q = \frac{2l_c}{c(L+T_0)}$$

is the cold-cavity photon lifetime, L is the round-trip loss and can be expressed as $L = 2\delta l$, δ is the internal loss per unit length in the laser gain medium, and l_c is the optical length of the resonator, T_0 is the output coupler transmission.

From Eq. (7), the spatial distribution of the population inversion density is given by

$$\Delta N(r,z) = \frac{W_p\tau(N_{tot})\, r_p(r,z) - f_{low}N_{tot}}{1 + \frac{c\tau(N_{tot})\sigma}{n}\Phi\phi_L(r,z)}\,. \tag{9}$$

Substitute the population inversion density given in Eq. (9) into Eq. (8), an implicit relationship between the pump power P_0 and the total laser power P_c inside the cavity can be expressed as

$$4\pi l\sigma\int_0^l\int_0^\infty \frac{\tau(N_{tot})\,\frac{P_0\eta_a}{h\nu_p} r_p(r,z) - f_{low}N_{tot}}{1 + \frac{\tau(N_{tot})\sigma}{n}\frac{2nlP_c}{h\nu_L}\phi_L(r,z)} \times \tag{10}$$

$$\times\phi_L(r,z) r dr dz = L + T_0\,.$$

When the spatial distributions of the pump power and laser power inside the cavity Eq. (3) and Eq. (4) are substituted into Eq. (10), Eq. (10) can be rewritten as

$$\frac{8\sigma}{w_{L0}^2}\int_0^l\int_0^\infty \frac{\Xi\exp\left(\frac{-2r^2}{w_{L0}^2}\right) r dr dz}{1 + \frac{4P_c\tau(N_{tot})\sigma}{h\nu_L\pi w_{L0}^2}\exp\left(\frac{-2r^2}{w_{L0}^2}\right)} = L + T_0\,. \tag{11}$$

where

$$\Xi = \tau(N_{tot})\frac{2\alpha P_0}{h\nu_p\pi w_{p0}^2}\exp\left(\frac{-2r^2}{w_{p0}^2}\right) \times$$

$$\times\{\exp(-\alpha z) + \exp[-\alpha(2l - z)]\} - f_{low}N_{tot}\,.$$

Eq. (11) can be simplified by integrating over the length of the gain medium, then

$$\frac{8\sigma}{w_{L0}^2}\int_0^\infty \frac{\tau(N_{tot})\,\frac{2P_0}{h\nu_p\pi w_{p0}^2}\exp\left(\frac{-2r^2}{w_{p0}^2}\right)\eta_a - f_{low}N_{tot}l}{1 + \frac{4P_c\tau(N_{tot})\sigma}{h\nu_L\pi w_{L0}^2}\exp\left(\frac{-2r^2}{w_{L0}^2}\right)} \times$$

$$\times\exp\left(\frac{-2r^2}{w_{L0}^2}\right) r dr = L + T_0\,. \tag{12}$$

Let $x = 2r^2/w_{L0}^2$, $a = w_{L0}^2/w_{p0}^2$, and $y = \exp(-x)$, then Eq. (12) becomes

$$2\sigma \int_0^1 \frac{\tau\left(N_{tot}\right)\frac{2P_0\eta_a}{h\nu_p\pi w_{p0}^2}y^a - f_{low}N_{tot}l}{1+\frac{4P_c\tau(N_{tot})\sigma}{h\nu_L\pi w_{L0}^2}y}dy = \tag{13}$$

$$= L + T_0$$

in Eq. (13), if $P_c = 0$, the corresponding P_0 is the pump threshold P_{th}:

$$P_{th} = \frac{L + T_0 + 2\sigma f_{low}N_{tot}l}{\int_0^1 \tau(N_{tot})\frac{4\eta_a\sigma}{h\nu_p\pi w_{p0}^2}y^a dy} = \tag{14}$$

$$= \frac{h\nu_p\pi w_{p0}^2\left(a+1\right)\left(L + T_0 + 2\sigma f_{low}N_{tot}l\right)}{4\eta_a\tau(N_{tot})\sigma}.$$

3. Numerical simulation and predictions

The laser model proposed above was used to calculate the temperature dependent laser performance of diode laser pumped Yb^{3+}:YAG microchip lasers [4] by taking temperature dependent stimulated emission cross section and the thermal population distribution of Yb:YAG crystal into account. The parameters of the laser cavity and Yb:YAG laser material are listed in Table 1. The stimulated emission cross section, σ and the thermal population fraction

Parameters	Value
λ_p	940 nm
λ	1030 nm
w_{p0}	90 μm
w_{L0}	67 μm
P_0	0.58 W
T_0	0.15
δ	0.002 cm^{-1}
l	1 mm
C_0	39 at.%

Table 1 Values of the parameters used in the numerical simulation for Yb:YAG microchip lasers taken from [4]

T, K	P_{in}, W	P_{out}, mW		P_{th}, mW		Slope efficiency, %	
		Exp.	Cal.	Exp.	Cal.	Exp.	Cal.
70	0.58	430	420	120	54	90	80
100	0.58	380	392	145	78	82	79
130	0.58	320	332	190	126	78	74
150	0.58	225	261	215	192	64	69
180	0.58	50	100	419	390	30	53

Table 2 Comparison of calculated and experimental results for the Yb:YAG microchip laser

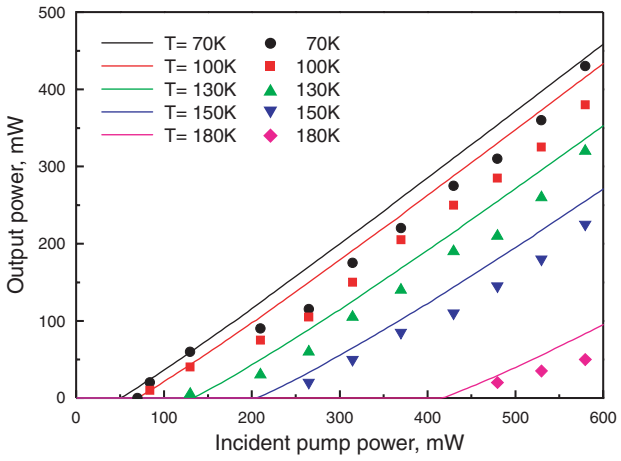

Figure 1 (online color at www.lphys.org) Output power of 25 at.% Yb:YAG microchip laser as a function of incident pump power at different temperatures, the length of Yb:YAG crystal is 1 mm, the output coupler transmission is 15%. The solid symbols show the experimental data, the lines show the numerical simulations

f_{low} and f_{up} of Yb:YAG crystal are strongly dependent on the temperature [2]. The relationship between the stimulated emission cross section of Yb:YAG crystal and temperature can be described as [2]

$$\sigma(T) = 2 + \frac{10.5}{1+\exp\left(\frac{T-131.6}{52}\right)} \times 10^{-20}\ \mathrm{cm}^2\,.$$

The temperature of Yb:YAG microchip is calculated according to Eq. (6). The experimental and calculated results of the diode laser pumped Yb^{3+}:YAG microchip laser at different cooling temperature are listed in Table 2, the experimental data are quoted from [4]. In this table, $P_{abs} = P_0$ and $P_{out} = P_cT_0$ represent the incident pump power and the output power, respectively. From Table 2, we can see that the numerical simulation of diode laser pumped 25 at.% Yb^{3+}:YAG laser is in good agreement with those of the experiments. The numerical simulation of the output power as a function of the incident pump power for diode laser pumped 25 at.% Yb:YAG microchip laser with 1 mm gain medium length and 0.15 output coupler transmission is shown in Fig. 1. The differences between the calculated and the experimental results shown in Table 2 and Fig. 1 may be caused by the following factors which were not taken into the consideration in the laser model: the optical inhomogeneity of the gain medium, the distribution variation of the absorbed pump power along the pump direction inside the gain medium according to Lambert-Beer law, the other loss of the laser cavity, etc. The thermal effect introduced by the absorbed pump power inside the gain medium enhances the vibration of the crystalline lattices and it will reduce the quantum efficiency of the luminescence and increase the linewidth of the luminescence spectrum, which will increase the pump power threshold and

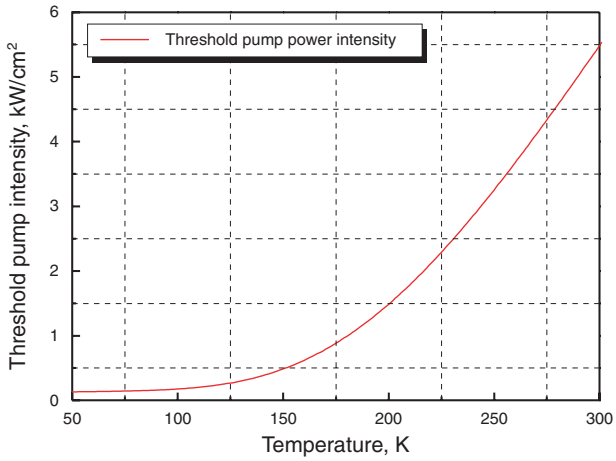

Figure 2 (online color at www.lphys.org) The temperature dependent pump power intensity threshold for Yb:YAG microchip laser

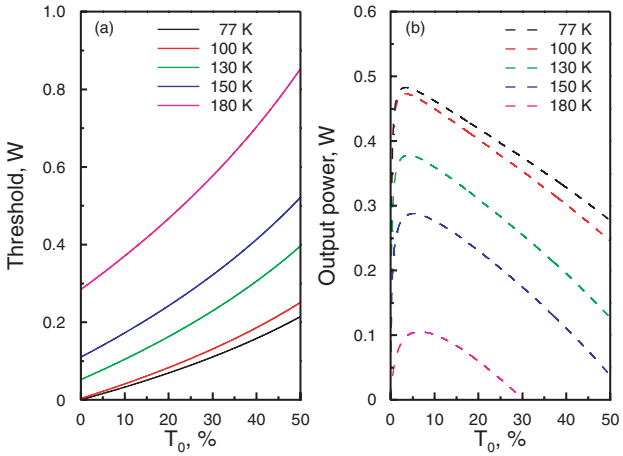

Figure 3 (online color at www.lphys.org) (a) The pump power threshold and (b) output power as a function of transmission of output coupler at different temperature. The incident pump power was set to be 0.58 W. The solid lines show the pump power threshold, the dashed lines show the output power

decrease the efficiency of the laser performance. For the end-pumped microchip lasers, the absorbed pump power inside the gain medium is not uniformly distributed and decreases from the entrance of the pump power to the exit of the pump power, so the deformation inside the gain medium will be induced, which will result in more interaction between the active ions and the impurities, therefore the loss of the crystal will increase. In most cases, the radius of the pump power adopted in the numerical calculations is not exactly the same as that in the laser experiments because there is measurement error when the radius of the pump power was measured. Therefore, there will be some discrepancies between the calculated results and the experimental results.

Fig. 2 shows the temperature dependent threshold pump power intensity. The pump power intensity increase dramatically with temperature when the temperature is above 120 K, this is caused by the thermal distribution of the low-laser-level population and the decrease of the stimulated emission cross section of Yb:YAG crystal. To obtain efficient laser operation from 200 K to room temperate, the high pump power density is required. This result agrees with the high pump power intensity for Yb doped laser crystal. The pump power intensity in [4] is very low (2.3 kW/cm^2 at maximum pump power), there is no laser oscillation when the temperature is higher than 180 K.

From Eqs. (13) and (14) we can see that the transmission of the output coupler has the effect on the pump power threshold and the output power of diode laser pumped Yb:YAG microchip lasers. The pump power threshold is proportional to the transmission of the output coupler, and there should be an optimizing transmission for the highest output power under certain pump power. Fig. 3 shows the pump power threshold and the output power of 25 at.% Yb:YAG crystal with 1-mm thickness under 0.58-W pump power as a function of the transmission of the output coupler at different temperatures. The pump power threshold increases with the transmission of the output coupler, the threshold pump power increases with temperature for the same transmission of the output coupler, the higher the temperature, the higher the pump power threshold. There is an optimal transmission of output coupler for achieving highest output power at different temperature, and the optimal transmission for this configuration increases from 3.5% to 7% with temperature from 70 K to 180 K. The highest output power is about 483 mW at 77 K, and 105 mW at 180 K, corresponding optical-to-optical efficiency is 83.3%, 18.1% respectively.

The laser performance of Yb:YAG microchip lasers strongly depends on the doping concentration of Yb^{3+} ions and the thickness of the laser medium at certain temperature. Fig. 4 (a) shows the pump power threshold as a function of the thickness for different doping concentration of the Yb^{3+}:YAG crystal at 70 K, the internal loss per unit gain medium length is adopted to be 0.002 cm^{-1} as mentioned in [8], the transmission of the output coupler is set to be 0.05, the incident pump power is 0.58 W. The threshold decreases dramatically with the increase of the length of gain medium when the gain medium length is shorter than 0.25 mm as shown in Fig. 4a, the lower pump power threshold can be achieved when the crystal length is longer than 1.25 mm, 0.75 mm, 0.3 mm, and 0.3 mm for 5 at.%, 10 at.%, 25 at.%, and 40 at.% doping concentration, respectively. The pump power threshold nearly does not increase with the doping concentration of the gain medium when the length of gain medium is greater than 1.25 mm because thermal population distribution effect of lower laser level can be neglected at low temperature. The

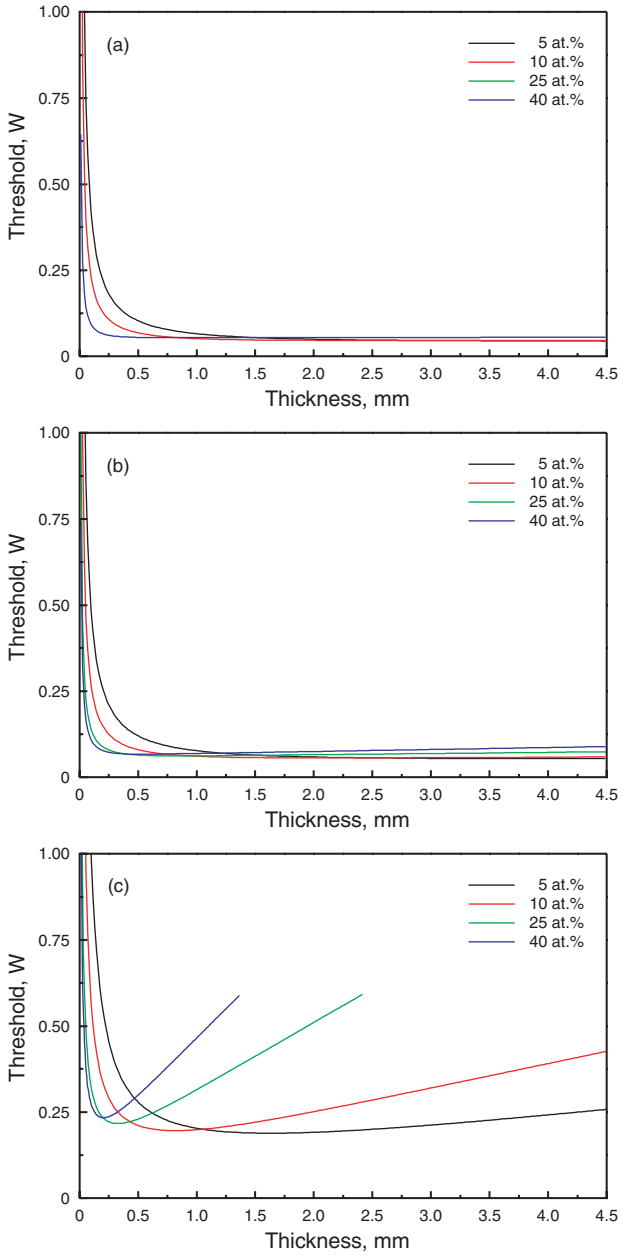

Figure 4 (online color at www.lphys.org) The pump power threshold as a function of thickness for different doping concentration of Yb:YAG crystal at (a) 70 K, (b) 100 K, and (c) 180 K

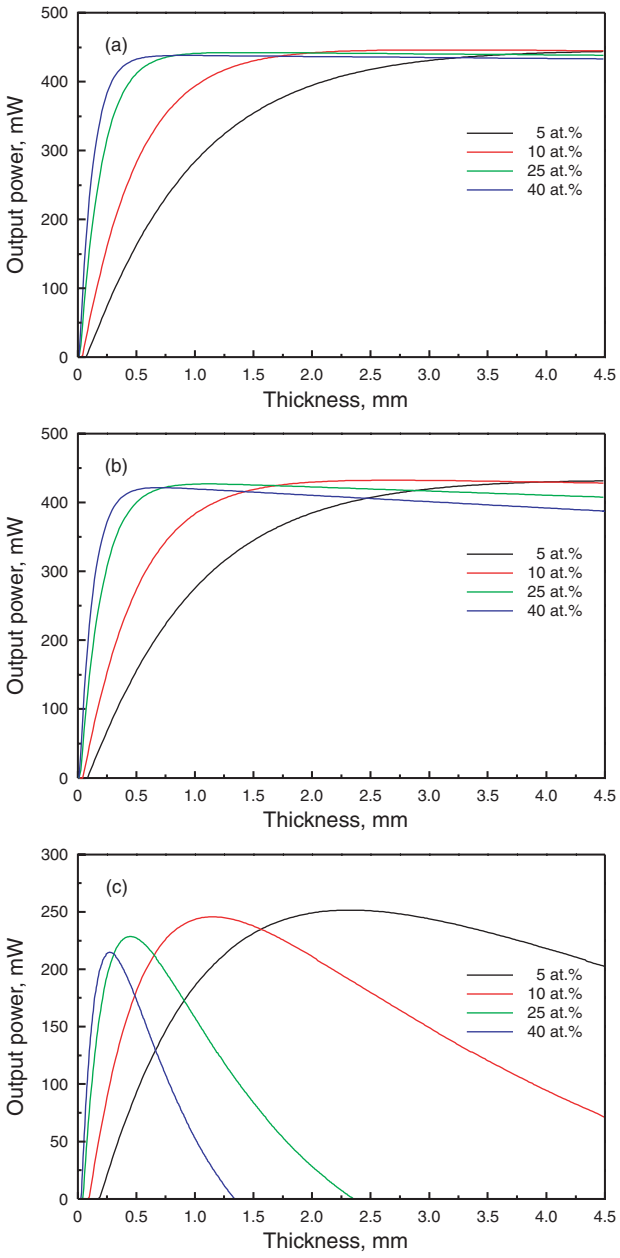

Figure 5 (online color at www.lphys.org) The output power as a function of thickness for different doping concentration of Yb:YAG crystal at (a) 70 K, (b) 100 K, and (c) 180 K

same situation for the pump power threshold was also observed when the laser was working at 100 K (as shown in Fig. 4b). With further increase working temperature, the pump power threshold strongly depends on the thickness and the concentration of Yb:YAG crystal (as shown in Fig. 4c). There is an optimum thickness of the Yb:YAG for different doping concentration to obtain the lowest pump power threshold. The optimum thickness of Yb:YAG crystal are 1.5 mm, 0.8 mm, 0.3 mm, and 0.2 mm for 5 at.%, 10 at.%, 25 at.%, and 40 at.% Yb doping concentration at 180 K. The output power of Yb^{3+}:YAG laser as a function of the thickness of the gain medium for different doping concentrations at 70 K is shown in Fig. 5a. The maximum output power can be achieved with 4.5 mm, 2.5 mm, 1 mm, and 0.8 mm thickness for 5 at.%, 10 at.%, 25 at.%, and 40 at.% respectively. Nearly the same situation keeps for the Yb:YAG laser working at 100 K (as shown in Fig. 5b) expect for the output power of highly doped Yb:YAG de-

creases a little with increase of the thickness of the gain medium which is caused by the thermal population distribution in highly doped Yb:YAG crystal becoming significant which can not be ignored. When Yb:YAG laser works at 180 K or above, the thermal population distribution have very significant effect on the laser performance (as shown in Fig. 5c). There is an optimum thickness for different doping concentration to obtain the maximum output power. The optimum thickness are 2.3 mm, 1.2 mm, 0.45 mm, and 0.27 mm for 5 at.%, 10 at.%, 25 at.%, and 40 at.% Yb doping concentration, respectively. The maximum output power decreases with the doping concentration, which shows that concentration quenching effect and the reabsorption at the laser wavelength due to the thermal population distribution in highly doped Yb:YAG crystal on the laser performance is more strongly at higher temperature than that at lower temperature. From Fig. 4 and Fig. 5, the lower pump power threshold and higher output power can be achieved by using different combinations of the doping concentration and the thickness of the Yb:YAG crystal. The thicker gain medium with low concentration can be chosen to realize more uniform pump power distribution along the pump direction at low temperature.

The output power can be scaled by increasing the pump beam radium and the pump power and keeping the pump power intensity as constant which is smaller than the value of the thermal fracture limit. The scaling of the power have been demonstrated by increasing the pump power diameter at nitrogen temperature [5]. The incident pump power is 135 W, the diameter of the pump beam is 1.5 mm, the transmission of the output coupler is 28%, a 0.6 mm thickness Yb:YAG doped with 25 at.% Yb was used as a gain medium. The maximum output power is 75 W was achieved at an absorbed pump power of 106 W with single-pass pumping configuration. Taking these data into the previous equations, the output power as a function of the incident pump power is shown in Fig. 6, which is in good agreement with the experiment [5]. The optical-to-optical efficiency can be enhanced by using two-pass pumping configuration. The optical-to-optical efficiency of end-pumped microchip Yb:YAG laser as a functions of temperature and pump power intensity is shown in Fig. 7a. High efficient performance of microchip Yb:YAG laser can be realized by working at low temperature or being pumped with high intensity pump power. The temperature has great effect on the laser performance of Yb:YAG laser, high efficient laser performance can be realized when Yb:YAG working below 160 K even with low pump power intensity, at the same time the thermal properties is better of Yb:YAG at low temperature than at room temperature. Yb:YAG laser working at low temperature provides more flexibilities for obtaining efficient laser output because the optical property such as stimulated emission cross section is larger and the thermal properties are better than those at room temperature. Fig. 7b shows the output power as a function of pump beam diameter at different temperatures when the pump power intensity is kept as 8 kW/cm^2 with two-pass pumping configuration. The output power is

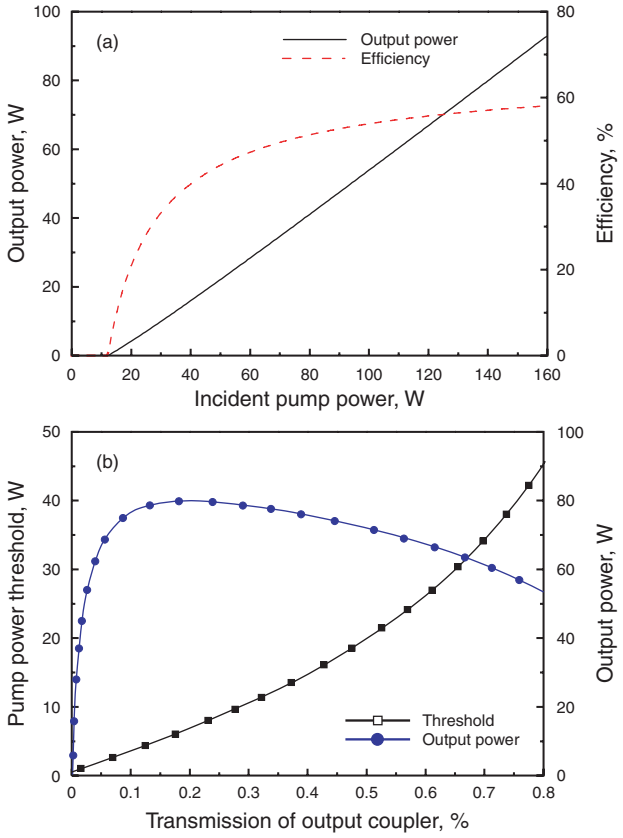

Figure 6 (online color at www.lphys.org) (a) The output power and optical-to-optical efficiency as a function of the incident pump power, (b) the pump power threshold and output power as a function of the transmission of the output coupler for Yb:YAG microchip laser cooling at nitrogen temperature. The transmission of the output coupler is 28%. The thickness of Yb:YAG is 0.6 mm

nearly proportional to the square of the pump beam diameter at different temperatures. The output power of Yb:YAG microchip laser increases with the decrease of the temperature at the same pump power diameter.

4. Conclusions

The theoretical model for CW Yb^{3+} doped YAG microchip lasers including the concentration quenching effect and temperature dependent emission cross section and the temperature dependent thermal population distribution is proposed based on the quasi-three-level-system. Other factors related to the output power of diode laser pumped Yb:YAG microchip lasers, such as the gain medium's thickness, the doping concentration of Yb^{3+} ions, the incident pump power, the transmission of the output coupler and the fluorescence lifetime of the upper level, are taken into account. The numerical simulation of

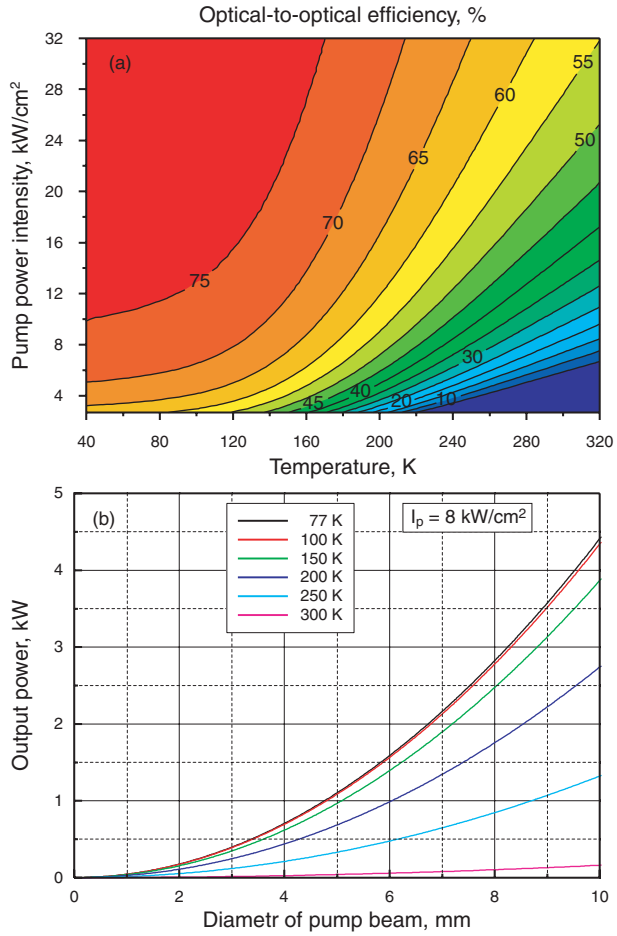

Figure 7 (online color at www.lphys.org) (a) The optical-to-optical efficiency of Yb:YAG microchip laser as a function of temperature and pump power intensity. The 0.6 mm Yb:YAG doped with 25 at.% Yb is used as gain medium, the transmission of the output coupler is 20%. (b) The output power of Yb:YAG microchip laser as a function of pump beam diameter at different temperature when the pump power intensity is 8 kW/cm^2

diode laser pumped Yb:YAG microchip laser at different temperature is in good agreement with those of the experiments. From the calculation of the pump power threshold and output power as functions of the thickness and the concentration of the gain medium at different temperature, the optimized relationship between the doping concentration and the thickness of the Yb:YAG crystal enables the microchip lasers have a relatively low pump power threshold and high efficient laser operation at a certain pump power level. The effect of decrease of the thickness will benefit for the thermal management for laser operation with high concentration Yb:YAG crystal as gain medium. The same output power can be achieved by using different concentration gain medium with relevant thickness. The optimized concentration for microchip laser operation should be over 10 at.%, and the optimized length of Yb:YAG microchip should be in the range of between 0.3 mm and 2 mm. The efficient laser performance of Yb:YAG laser can be realized by working at low temperature or using high pump power intensity. Low temperature operation of Yb:YAG laser provides more flexibilities for efficient laser design owing to the better optical and thermal properties of Yb:YAG at low temperature. The output power can be scaled by increasing the working area of the Yb:YAG gain medium.

Acknowledgements This work was supported by the 21st Century Center of Excellence (COE) program of Ministry of Education, Science and Culture of Japan.

References

[1] D.C. Brown, IEEE J. Quantum Electron. **33**, 861 (1997).
[2] J. Dong, M. Bass, Y. Mao, et al., J. Opt. Soc. Am. B **20**, 1975 (2003).
[3] D.J. Ripin, J.R. Ochoa, R.L. Aggarwal, and T.Y. Fan, Opt. Lett. **29**, 2154 (2004).
[4] T. Shoji, S. Tokita, J. Kawanaka, et al., Jpn. J. Appl. Phys. **43**, L496 (2004).
[5] S. Tokita, J. Kawanaka, M. Fujita, et al., Appl. Phys. B, in press.
[6] A. Giesen, H. Hugel, A. Voss, et al., Appl. Phys. B **58**, 365 (1994).
[7] C. Stewen, K. Contag, M. Larionov, et al., IEEE J. Sel. Top. Quantum Electron. **6**, 650 (2000).
[8] W. Kochner, Solid State Laser Engineering (Springer-Verlag, Berlin Germany, 1999).
[9] T. Taira, J. Saikawa, T. Kobayashi, and R.L. Byer, IEEE J. Sel. Top. Quantum Electron. **3**, 100 (1997).
[10] W.P. Risk, J. Opt. Soc. Am. B **5**, 1412 (1988).
[11] M.E. Innocenzi, H.T. Yura, C.L. Fincher, and R.A. Fields, Appl. Phys. Lett. **56**, 1831 (1990).
[12] T.Y. Fan and R.L. Byer, IEEE J. Quantum Electron. **23**, 605 (1987).
[13] T.Y. Fan and R.L. Byer, IEEE J. Quantum Electron. **24**, 895 (1988).